Study on The Influence of Spacing Between Bridge Piers on the Water Flow Characteristics in a 90° Curved Channel

Tingting Song, Xi Shi*, Hu Tao, Qianwen Jin, Yuanshun Huo

College of Civil Engineering, Lanzhou Jiaotong University, Lanzhou 730070, China

* Corresponding author. E-Mail: shixi103@163.com

Abstract. Using the RNG turbulence model and PISO algorithm, a 3D model of a 90° bend was constructed to analyze the influence of pier spacing on the flow characteristics in the bend. The study found that: ① The circulation structure is active in the low-flow region, with interactions between flow velocity and circulation. ②As s/d increases, the superposition effect of water flow weakens, reducing turbulence and vortex formation. ③ Along the depth direction, relative turbulent energy forms an inverted 'W' shape on both sides and an inverted 'S' shape at the central axis.

Keywords: Bend flow characteristics; circular end bridge piers; span-to-diameter ratio; bend circulation;

1 Introduction

In curved river channels, the construction of bridges is inevitable; however, the presence of bridge piers complicates flow patterns in the channel. Extensive domestic and international research has employed experimental and numerical simulation methods to investigate the influence of bridge piers on flow characteristics in curved channels, yielding fruitful results. Li et al.[1] examined local scouring under ice cover in an S-shaped channel with dual pier arrangements and observed that increasing the spacing between piers leads to a proportional increase in relative maximum scour depth. Ali-Asghar et al. [2] highlighted that turbulent flow around pier groups in curved channels is significantly influenced by spacing ratio, with a spacing ratio of 3 resulting in maximum bed shear stress. Yilmaz, Wang et al. [3-4] explored the impact of varying spacing between dual bridge piers on scour depth and established empirical formulas for predicting scour depth. In practical applications, circular end-shaped piers are widely utilized in engineering projects; Shi et al. [5], Gao Chenchen[6], etc., discovered that when circular end-shaped piers are installed in river channels, they effectively reduce water obstruction width and backwater height while mitigating flow disturbance.

Currently, most related studies focus on straight rivers, with relatively limited investigations into the influence of pier spacing on flow structures. Therefore, this study

G. Zhao et al. (eds.), *Proceedings of the 2024 6th International Conference on Civil Architecture and Urban Engineering (ICCAUE 2024)*, Advances in Engineering Research 262,
https://doi.org/10.2991/978-94-6463-688-8_22

investigates the relationship between pier spacing and hydraulic characteristics such as circulation structure and turbulence properties within a 90° bend channel to provide valuable insights for bridge pier design and river management.

2 Mathematical Modelling and Geometric Calculations

2.1 Control Equations

Compared with other turbulence models, the RNG $k-\varepsilon$ model can better handle flows with high strain rates and significant flow curvature. Therefore, in this study, the RNG $k-\varepsilon$ turbulence model is used for calculations. Its mathematical expression is as follows [7-9]:

the k equation is:

$$\frac{\partial(\rho k)}{\partial t}+\frac{\partial(\rho k u_i)}{\partial x_i}=\frac{\partial}{\partial x_j}\left[\alpha_k \mu_{\text{eff}}\frac{\partial k}{\partial x_j}\right]+G_k-\rho\varepsilon \tag{1}$$

the ε equation is:

$$\frac{\partial(\rho\varepsilon)}{\partial t}+\frac{\partial(\rho\varepsilon u_i)}{\partial x_i}=\frac{\partial}{\partial x_j}\left[\alpha_\varepsilon \mu_{\text{eff}}\frac{\partial \varepsilon}{\partial x_j}\right]+C_{1\varepsilon}^{*}\frac{\varepsilon}{k}G_k-C_{2\varepsilon}\rho\frac{\varepsilon^2}{k} \tag{2}$$

Here, $\mu_{\text{eff}}=\mu+\mu_{\text{t}}$; $C_{\mu}=0.845$; $\alpha_k=\alpha_\varepsilon=1.39$; $C_{1\varepsilon}=1.42$; $C_{2\varepsilon}=1.68$; $C_{1\varepsilon}^{*}=C_{1\varepsilon}-\eta(1-\eta/\eta_0)/(1+\beta\eta^3)$; $\eta_0=4.377$; $\beta=0.012$; $\eta=\left(2E_{ij}\cdot E_{ij}\right)^{1/2}\frac{k}{\varepsilon}$;

2.2 Working Condition Setting

Taking s/d=3 as an example, the physical model constructed is shown in Figure 1. The O point is taken as the origin of calculation. The model mainly consists of straight sections and curved sections, with a bending angle of 90°. The dimensions of the model are shown in Figure 1(a). At the bend apex at 45° from left to right (from convex side to concave side), three circular end-shaped piers are orthogonally arranged and labeled as 1#~3#, as shown in Figure 1. Four typical cross-sections are selected, as shown in Figure 1(b), and the calculation conditions and water flow parameters can be found in Table 1.

Table 1. Calculation conditions and model parameters

operating conditions	Wide B/m	s/m	*s/d*	*V*/(m/s)	Re/10^4
B1	0.8	0.08	2	0.25	4.29
B2	0.8	0.12	3	0.25	4.29
B3	0.8	0.20	5	0.25	4.29

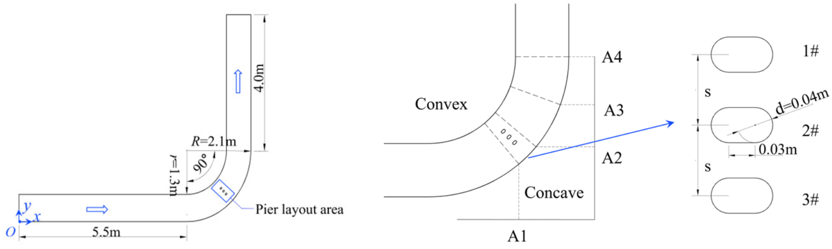

(a)Dimensions of Models (b)section view

Fig. 1. Curve model size and characteristic section diagram

2.3 Grid Division

In this paper, Mesh software is used to divide the grid. In order to ensure the controllability of node distribution, hexahedral structured mesh is used to divide the calculation region. In order to improve the calculation accuracy, the edge wall is encrypted, and the area near the water-gas interface is encrypted. Under different working conditions, the grid division principle is basically the same, totaling about 1.3 million, and its grid quality meets the calculation requirements, as shown in Figure 2.

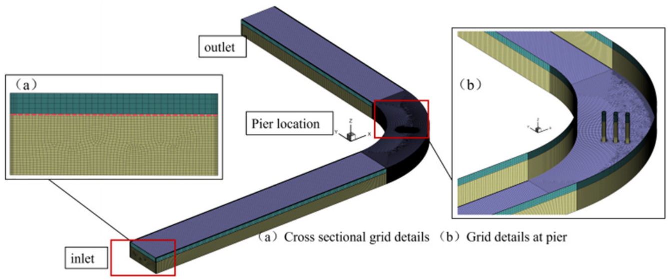

Fig. 2. Three-dimensional grid division diagram

2.4 Boundary Conditions

By using the finite volume method to discretize the governing equations, employing the RNG turbulence model, and selecting the PISO algorithm. The residual was set to 1×10^{-8}. In the calculation process, the boundary conditions are set as follows: (1) the inlet is divided into water phase (bottom) and gas phase (top) two layers, the water phase is set as the velocity inlet (V= 0.25m/s), the gas phase is set as the pressure inlet, and the free liquid surface is tracked by VOF method; ② The outlet is a mixed pressure outlet;

3 Calculation Results and Analysis

3.1 Circulation Structure

The Figure 3 shows the distribution of along-channel circulation structures under three different distance-to-diameter ratios of 2, 3, and 5. It can be observed that after water flows into the bend, circulation gradually forms and develops. Regardless of the spacing, there is a consistent change in the circulation structure at cross-section A4. At cross-section A5 behind the pier, a strong vortex structure appears. With an increase in distance-to-diameter ratio, the interaction between piers weakens, local velocity decreases, and vortex structures gradually separate and form complete ones, reducing turbulence and vortex formation in water flow. The circulation structure further develops into more fully developed ones near the bottom surface of convex bank at cross-section A7. At cross-section A9, regardless of different distance-to-diameter ratios, the circulation structures gradually converge to consistency. It can be found that areas with active circulation have relatively lower flow velocities. Once formed, circulations significantly alter momentum and energy distribution within sections thereby affecting dynamic balance of overall flow field.

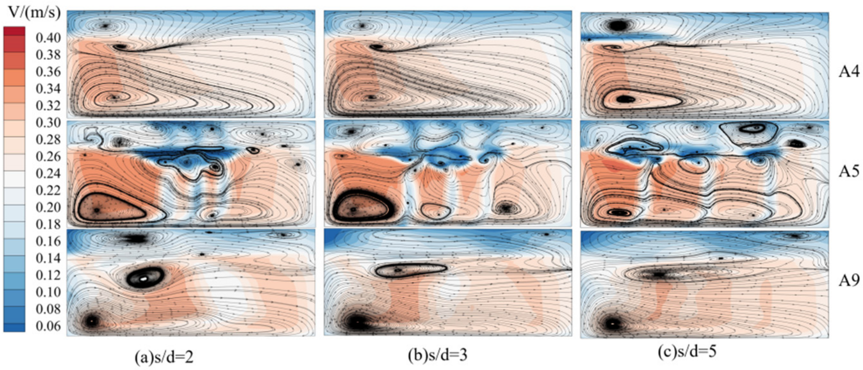

Fig. 3. Circulation structures at different sections are distributed along the way

3.2 Vertical Distribution of Turbulent Kinetic Energy

Turbulence kinetic energy is a physical quantity that characterizes the strength of turbulent turbulence and plays an important role in energy conversion and transfer[9]. Typical section C5 in the central layer z/h=0.5 is selected, and three survey lines are selected, which are respectively near the convex bank side (*L*/*B*=0.125), the central axis (*L*/*B*=0.50) and the concave bank side (*L*/*B*=0.875).

Figure 4 shows the relative trend of turbulent kinetic energy at section 5 of the pier after the failure under different spacing conditions. It can be observed that: as the aspect ratio increases, $K_{s/d=5}>K_{s/d=3}>K_{s/d=2}$ at the convex and concave sides of section C5; the relative turbulent kinetic energy along the water depth direction shows an inverted "W" distribution pattern, with higher turbulent kinetic energy regions appearing near the bottom surface ($z/h < 0.1$) and near the water surface ($z/h > 0.9$). At the mid-axis position, $K_{s/d=2} > K_{s/d=3} > K_{s/d=5}$, which is opposite to the convex and concave sides. When s/d =2, the water flow is the most turbulent; the relative turbulent kinetic energy shows a trend of first decreasing and then increasing along the water depth direction, presenting an inverted "S" distribution pattern, and the turbulence is greater than that on the two sides of the bend.

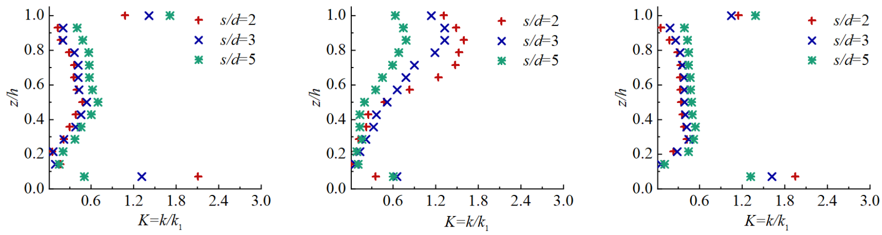

Fig. 4. Variation trend of the relative turbulent kinetic energy of C5 section along water depth direction

4 Conclusion

The article compares and analyzes the changes in circulation structure and turbulent kinetic energy with distance-to-diameter ratios of 2, 3, and 5. The following conclusions are drawn: (1) Regions with more circulation have lower water flow velocity; (2) With the increase of s/d, the superposition effect of water flow weakens, forming complete vortex structures and reducing turbulence and vortex formation in the water flow; (3) Along the depth direction, relative turbulent kinetic energy exhibits a reverse "W" shape on both sides with a reverse "S" shape at the central axis, which varies with changes in distance-to-diameter ratio.

5 Discussion

In bridge design and construction, the spacing between piers has a significant impact on flow turbulence. A smaller spacing may result in noticeable stacking effects, while a larger spacing can lead to severe scouring of the riverbed and pier foundations. Therefore, the optimal ratio of pier spacing to diameter is 3.

References

1. LI Zhicong, WANG Jun, SUI Jueyi, et al. Channel Bed Deformation around Double Piers in Tandem Arrangement in an S-Shaped Channel under Ice Cover[J]. Water, 2023, 15(14): 1-13.

2. Ali-Asghar Beheshti Behzad, et al. Numerical simulations of turbulent flow around side-by-side circular piles with different spacing ratios[J]. International Journal of River Basin Management, 2017, 15(2): 227-238.
3. Yilmaz M ,Yanmaz M A ,Koken M . Clear-water scour evolution at dual bridge piers[J]. Canadian Journal of Civil Engineering, 2017, 44(4): 298-307.
4. Wang H, Tang H, Liu Q, et al. Local scouring around twin bridge piers in open-channel flows[J]. Journal of Hydraulic Engineering, 2016, 142(9): 1-8.
5. Shi X, Tan CB, Gong L, et al . Analysis of water and flow field characteristics of river diagonal bridge[J]. Sediment Research, 2024, 49(02): 1-8.
6. Gao CH, Cai CY, Zhang ZJ, et al. Study on water blocking performance of semicircular-end bridge piers in plain rivers[J]. Water Resources and Hydropower Engineering, 2021, 52 (S2): 269-274.
7. Zhou Z, Zeng C, Zhou J, et al. Numerical investigation on distribution characteristics of velocities at equal-width open-channel confluences[J]. Hydro-Science and Engineering, 2020, (01): 32-39 .
8. Liu SH, Liao WJ. Differential model of total flow and principle of minimum energy dissipation for laminar flow in open channel [J]. Engineering Journal of Wuhan University, 2019, 52 (09): 753-757+801.
9. Ran DJ, Wang WE, Hu XT et al. Analyzing hydraulic performance of trapezoidal cutthroat flumes[J]. Advances in Water Science, 2018, 29 (02): 236-244.